

		ISSN 0016-7037 Volume 75, Number 2 January 15, 2011			
Geochimica et Cosmochimica Acta JOURNAL OF THE GEOCHEMICAL SOCIETY AND THE METEORITICAL SOCIETY					
EDITING EDITOR: FRANK A. PEEKER		EDITORIAL ASSISTANT: KAREN KLEIN KAREN SCYER			
EDITORIAL MANAGER: LINDA THOMER		WORKSHOP: ROBERT H. NEEDLE, JR. PRODUCTION MANAGER: CHRIS AYER			
ASSOCIATE EDITORS:	ROBERT C. ALLEN ROBERT C. ALLEN YOSHIO ANDO CAROL ARONOW MARIKA BAU-MATHIEU LIANG G. BERNING TAMARA S. BISHOP JAY A. BRANDEN ALAN D. BRIDSON DAVID J. BRIDGES BRADLEY H. BROWN WILLIAM H. CARMY THOMAS CHAPPEL JON CHAPPEL ANDRÉ COHEN CHRISTOPHER J. DICKERSON	ZHONGQI DING JAMES FARQUHAR FRANCIS A. FERT EDMUND GARLAND SUSAN CHANSON ETIENNE N. GOSWAMI JEROME R. HEALY H. ROBERT HARVEY GORDON R. HELL GREGORY F. HERRING SUDIP R. HIRAJI JAMES HIRAJI TAMARA HIRAJI JUN-ICHIRO ISHIZUKA KAREN JARVIS KLAUS JARVIS	CHRISTIAN KOPPEL RUSDI KOPPEL SINDHU M. KRASNER S. KRISHNAMOORTHY ALEXANDER N. KRYZ GREGORY A. LAGAN JONAS LITZ THOMAS J. LIVING MICHAEL L. MACHENRY BERNARD MARY TOM MCCALLUM ANDRÉS MURDO MARTIN A. MURDO JACK J. MURPHY ALFONSO MUSTI BIRGO MEXER	HIROSHI NAGAIWA MARTIN NÖVAK PATRYA A. OTTAY ERIC H. OHLBERG EMERSON PAPPASABERDI SANDRA PIZZARELLO MARK RIBBISSON W. UWE RIEBERG PETER W. RIEBERG EDWARD M. RILEY KEVIN M. RILEY SARA S. RISSALL E. J. RYDQVIST TOMAS A. SCHAEFER JACQUES SCHIFF THOMAS J. SELL	JIAN S. SHENBERG DAVIES DONALD I. SPARKER DAPHNE A. SODERBERG MICHAEL J. TAYLOR PETER ULLICH DORIS VANDE DAVID J. WALKER ROBERT J. WALKER LILLIAN A. WALKER JOHN WARDLE BOB A. WOODLEY CHIN ZHANG
Volume 75, Number 2		January 15, 2011			
Articles					
J. Z. BANDYKA, D. E. ROSS, S. L. BRANTLEY, W. D. BURGOS: Compendium and synthesis of bacterial manganese reduction rates . . .	337				
I. DREISING, S. WEISS, C. HENNING, G. BERNHARD, H. ZANKER: Formation of uranium(IV)-silica colloids at near-neutral pH	352				
X. HAN, Y.-L. LI, J.-D. GU: Oxidation of As(III) by MnO ₂ in the absence and presence of Fe(II) under acidic conditions	368				
S. FRIEL, L. J. FAIRCCHILD, J. FOHLMEISTER, R. MOKANDI, C. SPÖTL, A. BOKSAYI: Carbon mass-balance modelling and carbon isotope exchange processes in dynamic caves	380				
M. C. DAVIS, D. J. WROBLOWSKI, J. ROBINOVITZ, S. L. BRANTLEY, K. T. MUELLER: Solubility and near-equilibrium dissolution rates of quartz in dilute NaCl solutions at 398–473 K under alkaline conditions	401				
T. RONCAL-HERBERO, E. H. OHLKERS: Does vascite control phosphate availability in acidic natural waters? An experimental study of vascite dissolution rates	416				
B. KISACKÉK, A. EISENBAUER, F. BOHM, E. C. HATHORNE, J. EREZ: Controls on calcium isotope fractionation in cultured planktic foraminifera, <i>Globigerinoides ruber</i> and <i>Globigerinella siphonifera</i>	427				
J. P. SACHS, V. F. SCHWAB: Hydrogen isotopes in diatomol from the Chesapeake Bay estuary	444				
J. WU, M. L. WELLS, R. REMBER: Dissolved iron anomaly in the deep tropical-subtropical Pacific: Evidence for long-range transport of hydrothermal iron	460				
T. FUJII, F. MOTONO, N. DAUFHAR, M. ABE: Theoretical and experimental investigation of nickel isotopic fractionation in species relevant to modern and ancient oceans	469				
R. P. BRUCKER, J. McMASSUS, S. SEVERMANN, J. OWENS, T. W. LYONS: Trace metal enrichments in Lake Tanganyika sediments: Controls on trace metal burial in lacustrine systems	483				
M. W. BOWLER, V. A. SAMARKIN, K. M. BOWLER, S. B. JOTE: Weak coupling between sulfate reduction and the anaerobic oxidation of methane in methane-rich seafloor sediments during <i>ex situ</i> incubation	500				
<i>Continued on outside back cover</i>					

This article appeared in a journal published by Elsevier. The attached copy is furnished to the author for internal non-commercial research and education use, including for instruction at the authors institution and sharing with colleagues.

Other uses, including reproduction and distribution, or selling or licensing copies, or posting to personal, institutional or third party websites are prohibited.

In most cases authors are permitted to post their version of the article (e.g. in Word or Tex form) to their personal website or institutional repository. Authors requiring further information regarding Elsevier's archiving and manuscript policies are encouraged to visit:

<http://www.elsevier.com/copyright>



Hydrogen isotopes in dinosterol from the Chesapeake Bay estuary

Julian P. Sachs*, Valérie F. Schwab¹

University of Washington, School of Oceanography, Box 355351, Seattle, WA 98195, USA

Received 25 March 2010; accepted in revised form 19 October 2010; available online 27 October 2010

Abstract

The hydrogen isotope ratio of the dinoflagellate sterol dinosterol (4 α ,23,24-trimethyl-5 α -cholest-22E-en-3 β -ol) was measured in suspended particles and surface sediments from the Chesapeake Bay estuary in order to evaluate the influence of salinity on hydrogen isotope fractionation. *D/H* fractionation was found to decrease by $0.99 \pm 0.23\%$ per unit increase in salinity over the salinity range 10–29 PSU, a similar decrease to that observed in a variety of lipids from hypersaline ponds on Christmas Island (Kiribati). We hypothesize that the hydrogen isotopic response to salinity may result from diminished exchange of water between algal cells and their environment, lower growth rates and/or increased production of osmolytes at high salinities. Regardless of the mechanism, the consistent sign and magnitude of dinosterol δD response to changing salinity should permit qualitative to semi-quantitative reconstructions of past salinities from sedimentary dinosterol δD values. © 2010 Elsevier Ltd. All rights reserved.

1. INTRODUCTION

The hydrologic cycle is a central component of the climate system that has proven difficult to reconstruct in the past and challenging to forecast into the future. For much of the globe that means that precipitation rates are largely unknown prior to the widespread use of weather satellites in the 1970s, and forecasts of changing precipitation patterns in the coming decades are highly uncertain (cf. Solomon et al., 2009). Though tree rings have been successfully used to reconstruct rainfall in temperate regions of continents (Cook et al., 1999, 2004) precipitation is often a second-order influence on ring width and density when compared to temperature (Briffa et al., 2002). Furthermore, trees in tropical and desert regions often do not produce annual rings, and some 75% of the surface of the planet is covered by ocean or ice where trees do not exist. Attempts to reconstruct hydrologic changes from the chemical and isotopic composition of seawater preserved in the fossil remains of carbonate plankton and corals have

evolved to the point where relatively large changes in hydrologic conditions can be discerned for the last few hundred years in the case of corals, and on millennial time-scale in the case of foraminifera, but the changes in seawater chemistry caused by hydrologic changes are relatively small, making for a low signal-to-noise ratio in carbonate-based paleohydrologic proxies. Such studies are also limited to the shallow-water tropics in the case of corals, and those regions of the ocean where carbonate preservation in marine sediments is good. Without long records of precipitation over large parts of the globe it is difficult to evaluate the significance of precipitation trends in recent decades.

A promising new tool for reconstructing hydrologic conditions in the past from virtually any location where plant or phytoplankton remains can be found is the hydrogen isotope ratio ($^2\text{H}/^1\text{H}$ or *D/H*) of lipids produced by plants, phytoplankton and cyanobacteria (Sauer et al., 2001; Huang et al., 2002; Englebrecht and Sachs, 2005; Schefuss et al., 2005; Pagani et al., 2006; Schouten et al., 2006; Pahnke et al., 2007; van der Meer et al., 2007, 2008; Zhang and Sachs, 2007; Sachse and Sachs, 2008; Sachs et al., 2009; Schwab and Sachs, 2009; Zhang et al., 2009). Since vascular plants transpire, and transpiration causes variable isotopic enrichment of leaf water that depends on several environmental parameters (Flanagan et al., 1991), lipids derived

* Corresponding author.

E-mail address: jsachs@u.washington.edu (J.P. Sachs).

¹ Present address: Max-Planck-Institute for Biogeochemistry, Hans-Knoell-Str. 10, 07745 Jena, Germany.

from phytoplankton and cyanobacteria are desirable targets for paleohydrologic reconstructions based on D/H ratios (Englebrecht and Sachs, 2005; Pahnke et al., 2007; van der Meer et al., 2007, 2008; Zhang and Sachs, 2007; Sachs et al., 2009).

Both laboratory (Englebrecht and Sachs, 2005; Schouten et al., 2006; Zhang and Sachs, 2007; Zhang et al., 2009) and field (Huang et al., 2002; Englebrecht and Sachs, 2005; Sachse and Sachs, 2008; Schwab and Sachs, 2009) studies demonstrate that the hydrogen isotope ratio (δD), of a wide range of algal lipids closely co-varies with the δD values of the water in which they were produced. Their substantial deuterium depletion relative to environmental water, which is typically about 100–350‰, depending on the algal species and type of lipid (Sessions et al., 1999; Sauer et al., 2001; Zhang and Sachs, 2007), is likely the result of several isotope fractionating steps that occur during lipid biosynthesis. The magnitude of this depletion can also be modified by certain growth and environmental conditions that are just starting to be evaluated (Schouten et al., 2006; Zhang and Sachs, 2007; Sachse and Sachs, 2008; Wolhowe et al., 2009; Zhang et al., 2009).

Salinity (Schouten et al., 2006; Sachse and Sachs, 2008), nutrient-limited growth rate (Schouten et al., 2006; Sachse and Sachs, 2008; Zhang et al., 2009), growth stage (Wolhowe et al., 2009), and temperature (Zhang et al., 2009) have all been shown to influence D/H fractionation expressed in algal lipids. The mechanisms by which these environmental and growth conditions cause changes in the isotopic composition of cellular lipids are not yet well understood, though a variety of hypotheses have been put forth by the authors of the individual studies, and by several other researchers investigating D/H fractionation in plants and algae (Estep and Hoering, 1980; Sternberg et al., 1984; Sternberg et al., 1986; Ziegler, 1989; Smith and Ziegler, 1990; Luo et al., 1991; Yakir, 1992; Schleucher et al., 1999; Sessions et al., 1999, 2002; Hayes, 2001; Schmidt et al., 2003; Kreuzer-Martin et al., 2006; Sessions, 2006; Smith and Freeman, 2006; Chikaraishi and Naraoka, 2007; Campbell et al., 2009; Schwab and Sachs, 2009; Zhang et al., 2009). What is clear is that multiple environmental parameters can influence D/H fractionation expressed in algal lipid δD values via the changes they exert on cellular metabolism, biochemical changes, and the primary photosynthetic processes.

Salinity has recently emerged as an important influence on hydrogen isotope ratios in phytoplankton and cyanobacteria. A decrease in D/H fractionation between environmental water and lipids was observed when salinity increased in both laboratory culture (Schouten et al., 2006) and field experiments (Sachse and Sachs, 2008). When Schouten et al. (2006) cultured the common oceanic haptophytes *Emiliania huxleyi* and *Gephyrocapsa oceanica* at salinities between 25 and 35 PSU, they observed a decrease in D/H fractionation between alkenones and water ($\alpha_{\text{alk/water}}$) of ca. 0.003 or 3‰ per salinity unit. A strong influence of salinity on D/H fractionation in lipids was also observed in saline and hypersaline ponds on Christmas Island, Republic of Kiribati, where δD values of cyanobacterial lipids increased by 100‰ as salinity increased from 14

to 149 PSU, and lake water δD values increased just 12‰ (Sachse and Sachs, 2008). Based on these results, lipid δD values are now being used to reconstruct paleosalinity variation in a wide range of marine and terrestrial settings (Pahnke and Sachs, 2006; van der Meer et al., 2007; van der Meer et al., 2008; Sachs et al., 2009). As alternative proxies for salinity are virtually non-existent, there is a great need to continue to develop our understanding of the ways in which salinity may influence the δD values of lipids.

In an effort to evaluate the influence of salinity on D/H fractionation as recorded by dinosterol (4 α ,23,24-trimethyl-5 α -cholest-22E-en-3 β -ol), a ubiquitous lipid in marine and continental waters that is produced by dinoflagellates, and the fidelity with which dinosterol records water δD values, we measured its hydrogen isotope composition along the salinity and water δD gradient of the Chesapeake Bay (CB) estuary in Maryland and Virginia, eastern USA.

2. ANALYTICAL PROCEDURES

2.1. Sample collection

Sediment and suspended particles were collected May 22–25, 2006, from the *R/V Kerhin* at 11 sites along the longitudinal central axis of the CB (Fig. 1b). Samples were collected at sites routinely visited by the Maryland and Virginia Chesapeake Bay Monitoring Programs (<http://www.chesapeakebay.net/>). Near-surface sediments were collected with a Van Veen sediment grab sampler. The upper 0–2 cm of greenish-yellow surface sediment was scraped off, bagged and immediately frozen at -20°C . Water and suspended particle samples were collected at multiple depths at each sampling site – typically 1, 3, 5, 10 and 20 m – by tubing attached to a conductivity-temperature-depth continuous profiling instrument (Hydrolab series 3, Hach Environmental, Loveland, CO, USA) and filtered through a pre-combusted 293 mm diameter glass fiber filter with a 0.7 μm nominal pore size (Whatman GF/F) that was subsequently frozen at -20°C . Water for hydrogen isotope analysis was collected with each filter and between stations. Surface water salinity and temperature were continuously measured with a flow-through system on board the vessel.

2.2. Lipid extraction and pre-treatment

The procedure for dinosterol extraction and purification was slightly modified from that in Smittenberg and Sachs (2007). *n*-C₃₇ alkane, 2-nonadecanone (C₁₉-ketone) and cholesterol (Sigma–Aldrich) were added as internal standards to freeze-dried sediment prior to extraction with an Accelerated Solvent Extractor (ASE-200, Dionex Corp., Sunnyvale, CA, USA). Each sample was extracted three times for 5 min with a mixture of dichloromethane and methanol, (DCM/MeOH, 9:1 v/v) in a nitrogen atmosphere (N₂) at a temperature of 150 $^{\circ}\text{C}$ and a pressure of 1500 p.s.i. The solvent was removed under a stream of nitrogen using a Turbovap system (Caliper, Hopkinton, MA, USA). The extracts were separated with column chromatography on

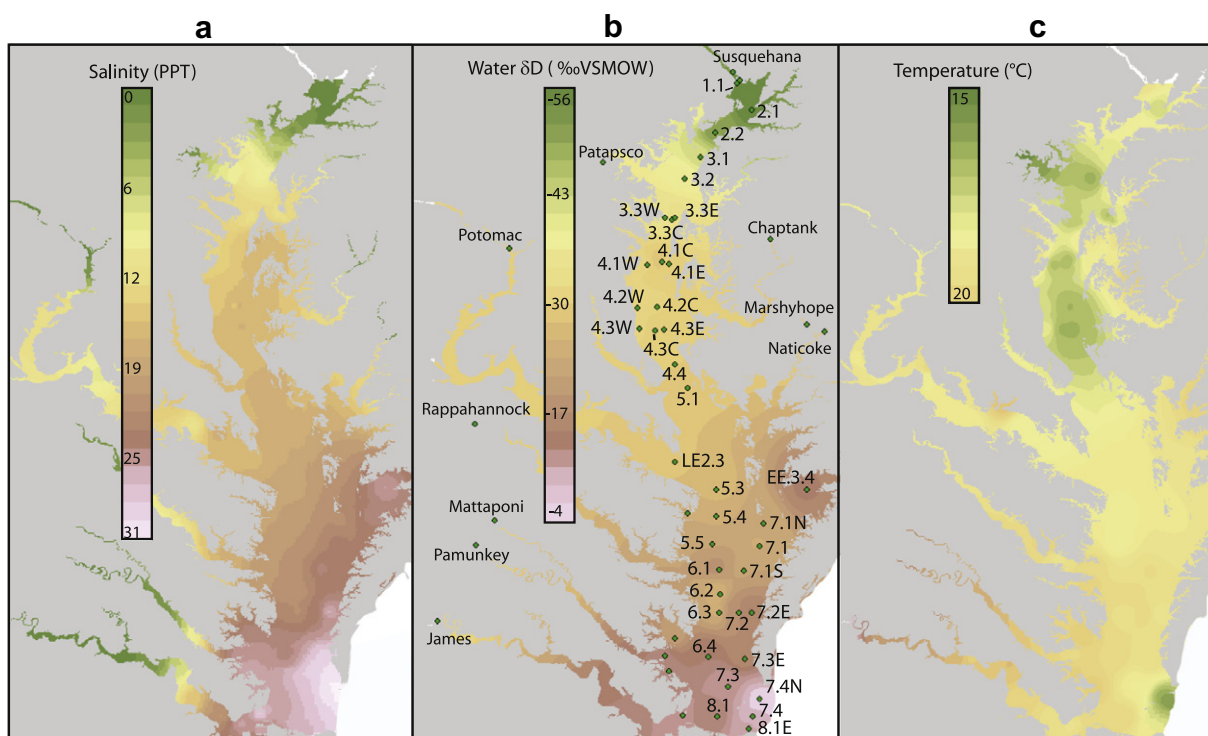


Fig. 1. Maps of the Chesapeake Bay showing surface (0–2 m) water (a) salinity, (b) δD_{water} values and sample locations, and (c) temperature. The station names and locations at which water samples were taken are indicated with diamonds. Maps were produced with ArcGIS Spatial Analyst, with inverse distance weighted output cell size of 0.001° , 131 salinity points, 105 water δD values, and 122 temperature points. Salinity and temperature data are from the Chesapeake Bay monitoring program (http://www.chesapeakebay.net/data_waterquality).

pre-combusted Al_2O_3 into four fractions. F1 was eluted with hexane/DCM (9:1, v/v) and contained hydrocarbons, F2 was eluted with hexane/DCM (1:1, v/v) and contained aromatic lipids and ketones, F3 was eluted with DCM/MeOH (1:1, v/v) and contained alcohols (including dinosterol) and F4 was eluted 100% MeOH and contained acids and polar lipids. Elemental sulphur was removed from F1 and F2 using activated Cu powder.

An aliquot of the F3 (alcohol) fraction was subsequently dried and re-dissolved in $10 \mu\text{L}$ of dry pyridine to which was added $10 \mu\text{L}$ of bis(trimethylsilyl)trifluoroacetamide (BSTFA, Sigma–Aldrich, St. Louis, MO, USA). The mixture was heated at 60°C for 30 min to convert alcohols into their corresponding trimethylsilyl ethers. The trimethyl silyl ether of dinosterol was identified by gas chromatography–mass spectrometry (GC–MS) using an Agilent (Santa Clara, CA, USA) 6890N gas chromatograph equipped with an Agilent 5983 autosampler, a split-splitless injector operated in splitless mode, and a HP-5ms column ($30 \text{ m} \times 0.32 \text{ mm i.d.} \times 0.25 \mu\text{m}$ film thickness, Agilent) interfaced to an Agilent 5975 quadrupole mass selective detector (MSD). After an initial period of 7 min at 70°C the column was heated to 150°C at $15^\circ\text{C}/\text{min}$, then at $6^\circ\text{C}/\text{min}$ to 320°C where it was held for 28 min. The MSD was operated in the electron impact mode at 70 eV, with a source temperature of 250°C , an emission current of 1 mA and with multiple-ion detection in the mass range from 50 to 700 amu at 2.28 scans/s.

Dinosterol was quantified with a Gas Chromatograph–Flame Ionization Detector (GC–FID). The Agilent 6890

GC was equipped with an Agilent 5983 autosampler and a programmable temperature vaporization inlet (PTV) operated in splitless mode. A 60 m Varian Chrompac CP-Sil 5 capillary column ($0.32 \text{ mm} \times 0.25 \mu\text{m}$) was used with helium as the carrier gas ($1.6 \text{ ml}/\text{min}$). The oven temperature was increased from 100° to 275°C at $40^\circ\text{C}/\text{min}$, then at $2^\circ\text{C}/\text{min}$ to 315°C where it was held for 37 min, and finally at $5^\circ\text{C}/\text{min}$ to 325°C where it was held for 5 min. Quantification of dinosterol was performed by comparing its integrated peak area to that of a cholesterol internal standard and a $n\text{-C}_{36}$ alkane external standard.

2.3. Dinosterol purification by HPLC–MS

Dinosterol was purified using high performance liquid chromatography–mass spectrometry (HPLC–MS) using a slightly modified procedure to that described in [Smittenberg and Sachs \(2007\)](#). Notable differences from this method are as follows. Prior to HPLC–MS the dinosterol-containing F3 fraction was re-dissolved in $100 \mu\text{L}$ of 10% of dichloromethane (DCM) in hexane pre-filtered through a $0.2 \mu\text{m}$ syringe filter (Acrodisc PSF, Pall Life Sciences, Ann Arbor, MI, USA). To improve separation and peak shape on the HPLC–MS, injection mass and volume were reduced to be less than $40 \mu\text{g}$ of dinosterol in $50 \mu\text{L}$ of solvent. The solvent gradient was also modified to streamline separation, using isocratic elution with a mixture of 15% DCM in hexane for 30 min at $1.5 \text{ mL}/\text{min}$ (followed by 100% DCM for 10 min at $2.0 \text{ mL}/\text{min}$ to clean the column). 2,2,4-trimethylpentane was used as the makeup flow to the

~2% MS split in favor of hexane, and detection of dinosterol was improved by monitoring the extracted ion m/z 411 as opposed to obtaining mass spectra in full scan mode.

Dinosterol retention time typically varied by $\sim \pm 10$ s, depending on the quantity and concentration in the injection. To ensure quantitative recovery of dinosterol and avoid *D/H* fractionation that occurs across the HPLC peak (Smittenberg and Sachs, 2007), while at the same time minimizing the contribution of contaminants that could co-elute with dinosterol during subsequent GC-irMS analyses, the fraction collector was used to acquire several 30-s-long fractions before and after the (expected) elution time of dinosterol. Any vial with ~2% or more of the total dinosterol as determined by HPLC-MS and/or GC-MS was added to the primary sample. Each sample was analyzed by GC-FID and GC-MS before and after the HPLC-MS treatment in order to quantify dinosterol and determine its recovery and purity.

2.4. Hydrogen isotope analyses of water

The hydrogen isotope compositions of water were determined by Thermal Conversion Elemental Analysis (TC/EA) (Thermo Scientific, Waltham, MA, USA) coupled to a Thermo DELTA V PLUS mass spectrometer. Water (2 μ L) was injected into a standard water-configured TC/EA pyrolysis reactor at a temperature of 1450 °C. The H_3^+ factor (Sessions et al., 2001) was determined daily and varied between 3 and 4. Water samples were analyzed with six replicate analyses, of which typically the first three analyses were omitted due to memory effects from the previous sample. H_2 with a known isotopic composition was used as a reference gas and the hydrogen isotope values were calibrated against in-house lab standards and Vienna Mean Ocean Water (SMOW), Greenland Ice Sheet Precipitation (GISP) and Light Antarctic Precipitation (SLAP) international standards. Hydrogen isotope ratios are reported using delta notation

$$\delta D = [(D/H)_{\text{sample}} / (D/H)_{\text{standard}} - 1] \times 100\% \quad (1)$$

The mean standard deviation for all samples was 0.7‰. In cases where errors on individual samples are reported in the text, the standard deviation of the replicate analyses is given.

2.5. Hydrogen isotope analyses of dinosterol

Purified dinosterol fractions were re-dissolved in 20 μ L of dry pyridine and acetylated by adding 20 μ L of acetic anhydride with a known hydrogen isotopic composition (Dr. Arndt Schimmelmann, Indiana University) and heating at 60 °C for 1 h. Acetylated dinosterol fractions were subsequently dried under a N_2 stream and dissolved in toluene containing a C_{37} *n*-alkane standard. Dinosterol was quantified by comparing its integrated peak on GC-FID to that of the *n*- C_{37} standard using the GC conditions described previously, re-dissolved in toluene, and brought to a concentration of 300–350 ng/ μ L of acetylated dinosterol in order to obtain optimal signal intensity on the GC-IRMS with a 1 μ L injection.

Dinosterol δD values were determined by GC-irMS on a Thermo DELTA V PLUS system (Thermo Scientific, Waltham, MA, USA) (Smittenberg and Sachs, 2007). The gas chromatograph (Trace Ultra, Thermo) was equipped with a split-splitless injector operated in splitless mode at 300 °C, a TRIPLUS autosampler (Thermo Scientific, Waltham, MA, USA), and a DB5 ms capillary column (60 m \times 0.32 mm \times 0.25 μ m, Agilent) programmed from 80 to 200 °C at 20 °C/min, then at 4 °C/min to 320 °C, and held at 320 °C for 30 min. Helium was used as the carrier gas under a constant flow of 1 ml/min. Compounds were pyrolyzed in an empty ceramic tube heated at 1420 °C that was activated by injecting 1 μ L of *n*-hexane. Samples of 1 μ L were co-injected with 1 μ L of a standard comprised of C_{34} and C_{38} *n*-alkanes with known hydrogen isotopic compositions (A. Schimmelmann, Indiana University, Bloomington, Indiana) bracketing the dinosterol peak, and concentrations were adjusted so that the peak areas were similar to that for dinosterol. Isotopic values were calculated with ISODAT software pack 2 (Thermo-Fisher, Bremen, Germany) using the two co-injected standards. We verified our chosen injection concentration with dilution tests in which dinosterol and co-injection standards were analyzed at varying concentrations to ensure that no peak-area related isotopic bias was being introduced (Polisar et al., 2009). Dinosterol δD values were corrected for the three carboxylic hydrogen atoms in the acetylated derivative by a mass balance calculation.

Instrument performance and the H_3^+ factor were determined daily using a tank of H_2 reference gas and a mixture of *n*-alkanes (*n*- C_{14} to *n*- C_{44}) with known δD values that had been determined by TC/EA-irMS. The *n*- C_{34} , and *n*- C_{38} standards used for δD corrections and added to the *n*-alkane mixture used in monitoring instrument performance were purchased from A. Schimmelmann (Indiana University, Bloomington, Indiana). The average difference between the δD values of *n*-alkanes measured by GC-irMS and TC/EA-irMS was 3.9‰ ($N = 165$ runs with 22 peaks = 3630 analyses). The H_3^+ factor remained below 4 and stable during the period in which the measurements reported here were conducted. Dinosterol δD values were typically measured in triplicate. The precision of dinosterol δD measurements, as determined by the pooled standard deviation (S_p), calculated from Eq. (1), of 31 samples, 30 of which were measured in triplicate, one in duplicate, was 2.6‰. Individual sample measurement errors are reported as the standard deviation of replicate analyses.

$$S_p = \sqrt{\frac{\sum_{i=1}^k ((n_i - 1)s_i^2)}{\sum_{i=1}^k (n_i - 1)}} \quad (2)$$

3. RESULTS

3.1. Chesapeake Bay water chemistry, hydrology and physical properties

The CB is a 300-km long, shallow and partially mixed estuary located in the Mid-Atlantic region of the United

States of America. The axial channel is 12–30 m deep and the Bay average 14 m in depth. Circulation in the CB is typical for an estuary, with a seaward flow of freshwater in the upper layers and an influx of seawater at depth. Consequently surface salinities increase from the head to the mouth of the Bay (Fig. 1a), and there is a strong vertical salinity gradient (cf. Table 1) (Schubel and Pritchard, 1986; Austin, 2004). Seasonal, inter-annual and low frequency salinity variations are modulated by freshwater discharges from the largest tributaries, the Susquehanna (48% of total freshwater flux), Potomac (33%) and James (13%) Rivers (Austin, 2004).

Multi-decade time series of monthly physical, chemical and biological parameters in CB have been performed by the Chesapeake Bay Monitoring Program (<http://www.chesapeakebay.net>) in an effort to evaluate the progression of eutrophication and anoxia caused by agricultural and industrial runoff (Officer et al., 1984; Cooper and Brush, 1991; Harding and Perry, 1997; Zimmerman and Canuel, 2000; Marshall et al., 2003; Marshall et al., 2005). A summary of the water chemistry of the main stem of the CB during the time of our sampling in May 2006 is as follows (http://www.chesapeakebay.net/data_waterquality). Spring 2006 was relatively dry with low freshwater discharge from the Susquehanna River. As a result, nutrient loading to the Bay was relatively low and the spring bloom event was relatively small. In May 2006, Chl *a* concentrations at 5 m water depth ranged from 1.07 to 31.4 $\mu\text{g L}^{-1}$, with minimum values at the mouth of the Bay and maximum values in the mid-Bay region. Dissolved inorganic nitrogen and phosphate ranged from 0.13 to 0.88 mg L^{-1} and from 5.0 to 21.7 $\mu\text{g L}^{-1}$, respectively, with both nutrients most abundant at the head of the Bay and least abundant at the mouth. Surface water (0–2 m) temperatures were between 14.9 and 20.1 °C (Fig. 1c). A weak thermocline existed, with

mean surface temperatures 1° to 2 °C higher than bottom water temperatures. Surface water (0–2 m) salinities increased from 0 PSU at the head of the Bay to 30.8 PSU at the mouth (Fig. 1a). The mid-section of the Bay was characterized by a strong halocline at approximately 8 m, with bottom water salinities as much as 15 PSU higher than surface salinities. Hypoxic (1–30% O₂ saturation) or anoxic conditions characterized the bottom waters in the mid-Bay area in May 2006.

3.2. Water δD values

One hundred and sixty-seven water samples collected at different depths along the N–S longitudinal transect of the CB (electronic annex) and 11 freshwater samples from CB tributaries (electronic annex) were analyzed for their hydrogen isotope composition. δD_{water} values spanned the range -56.8‰ to -3.8‰ over a salinity range of 0–30.8 PSU (Fig. 1b). The hydrogen isotope composition of water in CB tributaries ranged from -54.8‰ in the Susquehanna River on the north side of the drainage basin, to -29.6‰ in the Choptank and Marshhope Rivers on the east side of the drainage basin (electronic annex, Fig. 1b). A value of -27.3‰ was measured in the York River in a sample that is suspected to have contained some seawater. Three other river water samples suspected of containing some seawater are indicated in the electronic annex and omitted from Fig. 2. The δD values of CB water were linearly correlated with salinity ($\delta D_{\text{water}} = 1.63 \pm 0.04 \times \text{salinity} - 52.3 \pm 0.7$, $R^2 = 0.91$; Fig. 2), with uncertainties represented as the standard error of the slope and intercept of the regression. The observed relationship reflects fractionation due to evaporation toward more saline media and the mixing line between marine and freshwater (Craig, 1961; Craig and Gordon, 1965b).

Table 1

δD values of dinosterol in suspended particles from different depths in the Chesapeake Bay, along with the δD values and salinities of the water from which those particles were filtered, and the concentration of dinosterol in $\mu\text{g/g}$ dry weight of particulate material. δD values of all dinosterol and water samples are the average of 3 measurements, the standard deviations of which are listed. Station locations are mapped in Fig. 1b.

Stations	Depth (m)	Dinosterol conc. ($\mu\text{g/g}$)	δD_{dino} (‰ VSMOW)	Std. dev.	N	δD_{water} (‰ VSMOW)	Std. dev.	Salinity (PSU)	$\alpha_{\text{dino-water}}$	Std. dev.	$\epsilon_{\text{dino-water}}$	Std. dev.
CB3.3C	0–2	1.8	–329	3.1	3	–37.6	0.3	9.6	0.697	0.003	–303	3.2
CB3.3C	4–5	0.9	–331	2.1	3	–28.9	0.4	13.9	0.689	0.002	–311	2.2
CB4.2C	0–2	0.8	–328	0.1	3	–32.1	0.7	12.7	0.695	0.001	–305	0.5
CB4.2C	4–5	1.2	–327	3.0	3	–27.7	0.3	13.6	0.692	0.003	–308	3.1
CB4.2C	8–10	0.8	–317	1.4	3	–19.9	1.0	15.0	0.697	0.002	–303	1.6
CB4.2C	10–13	0.2	–298	0.8	3	–15.5	0.3	18.9	0.713	0.001	–287	0.8
CB4.4	0–2	2.0	–320	2.8	3	–28.0	0.4	11.7	0.690	0.003	–300	2.9
CB5.2	0–2	1.1	–312	2.2	3	–25.8	1.3	13.9	0.706	0.002	–294	2.4
CB5.3	0–2	0.9	–320	2.4	3	–28.5	0.9	14.6	0.700	0.003	–300	2.6
CB5.3	4–5	1.0	–323	2.8	3	–29.5	0.9	14.6	0.697	0.003	–303	2.9
CB5.3	8–10	0.2	–312	2.4	3	–27.3	1.1	15.3	0.707	0.003	–292	2.6
CB6.4	0–2	0.5	–308	1.2	3	–19.2	0.2	18.5	0.706	0.001	–294	1.2
CB7.3	0–2	1.3	–303	0.6	3	–15.3	1.0	20.5	0.707	0.001	–292	0.9
CB7.4 N	0–2	0.5	–301	1.2	3	–10.6	1.0	28.8	0.706	0.001	–294	1.4
CB7.4 N	4–5	0.8	–292	2.3	3	–11.4	1.1	29.7	0.716	0.002	–284	2.5
CB7.4 N	12	0.3	–291	2.0	3	–5.0	0.7	29.8	0.713	0.002	–287	2.1

$$\alpha_{\text{dino-water}} = (1000 + \delta D_{\text{dino}})/(1000 + \delta D_{\text{water}}); \epsilon_{\text{dino-water}} = (((\delta D_{\text{dino}} + 1000)/(\delta D_{\text{water}} + 1000)) - 1) \times 1000.$$

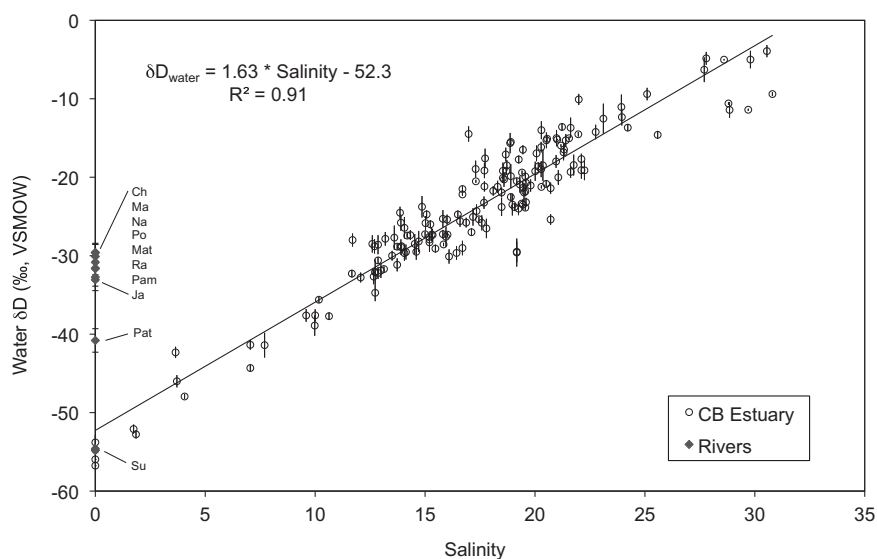


Fig. 2. Relationship between δD_{water} values and salinity in the Chesapeake Bay. Also plotted at zero salinity are the δD_{water} values of 11 of the larger rivers draining into the CB. Data and the rivers to which the abbreviations refer are listed in the [electronic appendix](#). The mean standard deviation of 3 analyses for every δD_{water} value was 0.7‰ .

3.3. Dinosterol distributions and δD values along the bay

Dinosterol ($4\alpha,23,24$ -trimethyl- 5α -cholest- $22E$ -en- 3β -ol) occurred in ample quantities for δD analyses in suspended particles from eight stations that had surface salinities between 9.6 and 28.8 PSU (Table 1), and in surface sediments from nine stations that had surface salinities between 7.7 and 30.8 PSU (Table 2). Dinosterol concentrations in suspended particles were between 0.2 and $2.0 \mu\text{g g}^{-1}$ dry weight of suspended particles (Table 1), and between 0.1 and $187 \mu\text{g g}^{-1}$ dry weight of sediment (Table 2), reaching a maximum in the middle Bay area.

Dinosterol δD values in suspended particles from surface water (0–2 m) were lowest ($-329 \pm 3\text{‰}$) at Stn. CB3.3C, where both salinity (9.6 PSU) and δD_{water} (-38‰) were lowest, and highest ($-301 \pm 1\text{‰}$) at Stn.

CB7.4N, where both salinity (28.8 PSU) and δD_{water} (-11‰) were highest (Table 1). Station locations, along with surface water salinities and δD_{water} values are shown in Fig. 1a and b. δD_{dino} values in suspended particles from subsurface waters in the 4–13 m depth range were usually higher than at 0–2 m and spanned the range $-331 \pm 2\text{‰}$ at 4–5 m at Stn. CB3.3C, to $-291 \pm 2\text{‰}$ at 12 m at Stn. CB7.4N (Table 1).

δD_{dino} values in the top 2 cm of sediment were lowest ($-333 \pm 2\text{‰}$) at Stn. CB3.2, above which (at 3 m water depth) both salinity (7.7 PSU) and δD_{water} (-41‰) were lowest, and highest ($-277 \pm 3\text{‰}$) at Stn. CB7.4N, above which (at 3 m water depth) both salinity (30.8 PSU) and δD_{water} (-9.4‰) were highest (Table 2). At the two stations (CB3.2 and CB5.3) where δD_{dino} values were measured in the 0–12 cm interval of sediment, in addition to the

Table 2

δD values of dinosterol in surface sediments from the Chesapeake Bay, and the δD values and salinities of the water at 3 m, corresponding to the zone of highest productivity. δD values of all dinosterol and water samples are the average of 3 measurements, the standard deviations of which are listed. Also shown are the concentration of dinosterol in $\mu\text{g/g}$ dry weight of sediment. Station locations are mapped in Fig. 1b.

Stations	Depth (cm)	Dinosterol conc. ($\mu\text{g/g}$)	δD_{dino} (‰ VSMOW)	Std. dev.	N	δD_{water} (‰ VSMOW)	Std. dev.	Salinity at 3 m (PSU)	$\alpha_{\text{dino-water}}$	Std. dev.	$\epsilon_{\text{dino-water}}$	Std. dev.
CB3.2	0–2	1.8	-333	1.8	3	-41.4	1.1	7.7	0.695	0.002	-305	2.0
CB3.2	0–12	3.7	-338	1.9	3	-41.4	1.1	7.7	0.691	0.002	-309	2.1
CB3.3C	0–2	4.3	-328	3.0	3	-37.6	0.7	10	0.698	0.003	-302	3.2
CB4.4	0–2	7.5	-316	4.9	3	-30.0	1.3	13.5	0.706	0.005	-294	5.1
CB5.2	0–2	187.4	-305	2.3	3	-28.8	0.6	12.7	0.715	0.002	-285	2.4
CB5.3	0–2	0.9	-305	2.8	3	-28.5	1.1	12.6	0.715	0.003	-285	3.0
CB5.3	0–12	1.1	-319	3.6	3	-28.5	1.1	12.6	0.700	0.004	-299	3.8
CB6.2	0–2	0.8	-300	1.3	3	-25.4	0.5	16	0.718	0.001	-282	1.4
CB6.4	0–2	0.6	-289	2.0	3	-19.2	0.9	18.7	0.724	0.002	-275	2.1
CB7.3	0–2	0.1	-285	2.8	3	-15.3	1.0	21.4	0.726	0.003	-274	2.9
CB7.4 N	0–2	0.2	-277	2.9	3	-9.4	0.4	30.8	0.730	0.003	-270	2.9

$$\alpha_{\text{dino-water}} = (1000 + \delta D_{\text{dino}})/(1000 + \delta D_{\text{water}}); \epsilon_{\text{dino-water}} = (((\delta D_{\text{dino}} + 1000)/(\delta D_{\text{water}} + 1000)) - 1) \times 1000.$$

0–2 cm interval, they were lower in the former ($-338 \pm 2\%$ vs. $-333 \pm 2\%$ at Stn. CB3.2, and $-319 \pm 4\%$ vs. $-305 \pm 3\%$ at Stn. CB5.3) (Table 2). Insufficient data exist to determine if this difference is representative of CB sediments, and therefore attributable to a temporal shift in δD_{dino} values.

Fractionation factors between individual dinosterol samples and water were calculated from the relationships:

$$\alpha_{\text{dino/water}} = (1000 + \delta D_{\text{dino}})/(1000 + \delta D_{\text{water}}) \quad (3)$$

$$\epsilon_{\text{dino/water}} = (\alpha_{\text{dino/water}} - 1) \times 1000 \quad (4)$$

(Sessions and Hayes, 2005). Uncertainty in the derived $\alpha_{\text{dino/water}}$ value is therefore the propagated uncertainty in the measurement error of both δD_{dino} and δD_{water} . These fractionation factors represent the ecosystem-integrated signal, as the dinosterol in our samples must certainly come from a variety of dinoflagellate species. Although no dinoflagellate culture experiments have been performed to determine the species-specific isotope effect, it is likely that significant differences exist given the large species influence observed in other culture data (Schouten et al., 2006; Zhang and Sachs, 2007). The dinosterol data considered here should therefore be viewed as apparent fractionation factors representing the average environmental signal.

The greatest isotope fractionation in particulate dinosterol was observed at station CB3.3C, where $\alpha_{\text{dino/water}} = 0.689 \pm 0.002$ and $\epsilon_{\text{dino/water}} = -311 \pm 2\%$ (Table 1). The smallest isotope fractionation in particulate dinosterol occurred at station CB7.4N where $\alpha_{\text{dino/water}} = 0.716 \pm 0.002$ and $\epsilon_{\text{dino/water}} = -284 \pm 3\%$. In surface sediments, an additional complication is that the sediments are clearly not derived exclusively from water of the exact same salinity and isotopic composition as those that were present in the overlying water column at the time of sampling. Nevertheless, there is benefit to comparing the results from particles and sediments as the sediments show the time-integrated signal, so we note that the greatest fractionation between sedimentary dinosterol and the overlying water at 3 m depth was at station CB3.2 where $\alpha_{\text{dino/water}} = 0.691 \pm 0.002$ and $\epsilon_{\text{dino/water}} = -309 \pm 2\%$, and the least apparent-fractionation was at station CB7.4N where $\alpha_{\text{dino/water}} = 0.730 \pm 0.003$ and $\epsilon_{\text{dino/water}} = -270 \pm 3\%$ (Table 2).

4. DISCUSSION

The Chesapeake Bay estuary provides an ideal environmental setting to evaluate (i) the fidelity with which algal lipids record the hydrogen isotopic composition of water and (ii) the influence of salinity and other properties on D/H fractionation in those lipids because the water δD values span a 53‰ range from -56.8% to -3.8% and the salinity spans a 31 PSU range from 0 to 31 PSU. Below we first discuss the isotope hydrology of the CB and identify possible influences on the relationship between water δD values and salinity. The next section addresses the relationship between water δD values and δD values in dinosterol from CB particles and sediments, demonstrating that this lipid faithfully tracks the isotopic composition of water. A discussion of the influence of salinity on D/H fractionation

in dinosterol follows, in which we show that D/H fractionation decreases as salinity increases, consistent with recent field and laboratory studies on other lipids (Schouten et al., 2006; Sachse and Sachs, 2008). Three hypotheses are subsequently posed to explain why salinity may exert a strong influence on D/H fractionation between dinosterol and environmental water.

4.1. Chesapeake Bay water δD values, salinity, and source water regions

The distribution of salinity and water δD values in the Chesapeake Bay is the result of both freshwater–seawater mixing as well as isotopic enrichment due to evaporation within the Bay. Each of these processes will produce slightly different relationships between water δD values and salinity (Craig, 1961; Dansgaard, 1964), so the degree to which one process may dominate locally over another may explain some amount of scatter in the relationship between the two ($R^2 = 0.91$, $N = 167$). The strength of the observed correlation argues against large variability in these effects, and the fact that the y -intercept plots between the measured δD values of the two major freshwater input sources, the Susquehanna and Potomac Rivers, suggests that CB hydrology is dominated by mixing as opposed to evaporative processes (Fig. 2). If the system was evaporation-dominated, the slope of the relationship between water δD values and salinity would differ due to the kinetic isotope effects associated with evaporation, which reduces the isotopic enrichment relative to evaporation-driven increases in salinity as compared to the isotopic enrichment and increasing salinity associated with freshwater–seawater mixing. As the balance between mixing and evaporative processes may not be constant through time, potential application of stable isotopes to any paleoclimate hydrology question must consider how the changing nature of these relationships through time might affect the reconstructed signal.

4.2. Producers of dinosterol in the Chesapeake Bay

The sterol composition of many dinoflagellates is dominated by $4\alpha,23,24$ -trimethyl- 5α -cholest- $22E$ -en- 3β -ol, commonly referred to as dinosterol (Boon et al., 1979; Withers, 1983; Alam et al., 1984; Volkman, 1986; Volkman et al., 1998; Leblond and Chapman, 2002). Of the 13 most common taxa of dinoflagellates (Dinophyceae) in the CB according to Marshall et al. (2006), 8 are known to produce dinosterol (*Akashiwo sanguinea*, *Gymnodinium* spp., *Gyrodinium* spp., *Heterocapsa triquetra*, *Prorocentrum minimum*, *Prorocentrum micans*, *Protoperidinium* spp., *Scrippsiella trochoidea*) and one (*Karlodinium micrum*) does not (Alam et al., 1984; Robinson et al., 1987; Mansour et al., 1999; Leblond and Chapman, 2002; Amo et al., 2007; Place et al., 2009). We were unable to find sterol data on the remaining 4 common dinoflagellate species (*Ceratium furca*, *Ceratium lineatum*, *Cochlodinium polykrikoides*, and *Heterocapsa rotundata*), but data on species closely related to 3 of these 4 suggest that one of them is likely to produce dinosterol (*H. rotundata* because *Heterocapsa niei*, *Heterocapsa pygmaea* (Leblond and Chapman, 2002) and *H. triquetra*

(Alam et al., 1984) produce it) and two are not (*C. furca* and *C. lineatum* because *Ceratium furcoides* does not (Robinson et al., 1987)). We thus expect that 9 of the 13 most common dinoflagellate taxa in the CB produce dinosterol, 3 probably do not, and one (*C. polykrikoides*) remains unknown.

Though dinosterol is produced in minor amounts by a small number of other phytoplankton, such as the marine diatom *Navicula speciosa* (Volkman et al., 1993) and Prymnesiophytes of the genus *Pavlova* (Volkman et al., 1990), these phytoplankton are uncommon in the Bay (Marshall et al., 2005). The ubiquity of dinosterol in lacustrine and marine settings and relative recalcitrance to chemical and biological degradation has prompted its widespread use as an indicator (biomarker) of dinoflagellates in both marine and lake sediments (Robinson et al., 1984; Schubert et al., 1998; Ishiwatari et al., 1999; Hanisch et al., 2003; Menzel et al., 2003; Calvo et al., 2004; Theissen et al., 2005).

The 13 most common species of dinoflagellates in the CB represent a substantial fraction of the total phytoplankton assemblage (Marshall et al., 2006). Of the species present, six are found throughout the bay, while the other seven are limited to either freshwater/oligohaline settings or mesohaline/polyhaline regions. Although these results are presented in the context of salinity regimes, there is no indication from these data that the dinoflagellate assemblages in the Bay vary gradually as a function of the salinity gradient. The seasonal phytoplankton succession is often initiated by an early spring bloom of dinoflagellates comprised primarily of *H. rotundata* and *S. trochoidea* in the freshwater/oligohaline regions, and *H. rotundata*, *S. trochoidea*, *H. triquetra*, *Gymnodinium* spp., and *P. minimum* in the mesohaline/polyhaline regions (Marshall et al., 2005). In summer, dinoflagellates, and *H. rotundata* in particular, comprise a substantial fraction of the phytoplankton community in the Bay, with significantly higher abundances and total biomass than in spring (Malone et al., 1991; Marshall et al., 2005). The phytoplankton assemblage during winter and autumn is generally dominated by diatoms, in particular *Skeletonema costatum* (Marshall, 1980), with varying abundances of cryptomonads and dinoflagellates (especially *Katodinium rotundatum* and *H. triquetra*) (Marshall and Nesius, 1996).

4.3. Relationship between δD_{dino} and δD_{water}

Dinosterol δD values and water δD values in the CB were highly correlated, with a higher slope and intercept in surface sediments ($\delta D_{\text{dino}} = 1.91 \pm 0.15 \times \delta D_{\text{water}} - 256 \pm 4$, $R^2 = 0.95$, $N = 11$) than in suspended particles ($\delta D_{\text{dino}} = 1.35 \pm 0.15 \times \delta D_{\text{water}} - 283 \pm 4$, $R^2 = 0.86$, $N = 16$) (Fig. 3a). Uncertainties in these and all subsequent regression analyses are given as the standard errors of the slopes and intercepts. Since dinoflagellates in the CB occur predominantly in the summer months (Malone et al., 1991; Marshall et al., 2005), and we sampled the Bay in late spring when runoff rates are high compared to the summer, higher dinosterol δD values in surface sediments relative to particles most likely represent the long-term (i.e., 1–

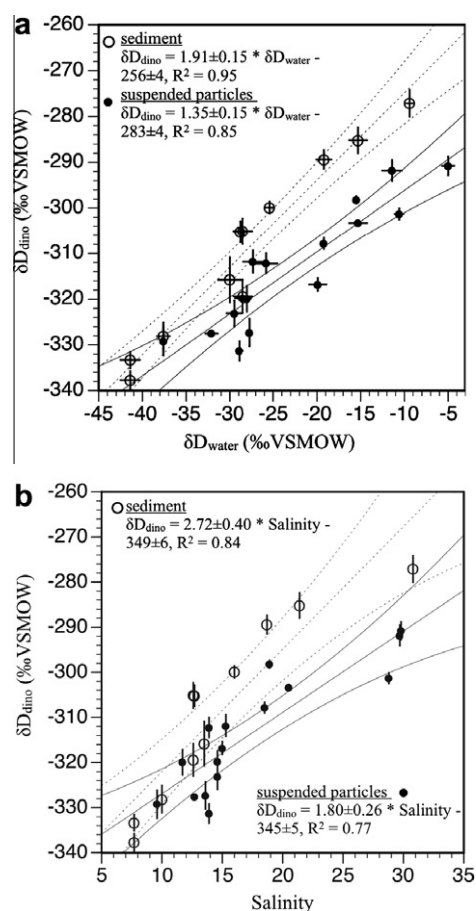


Fig. 3. Relationship between δD_{dino} and (a) δD_{water} and (b) salinity in suspended particles (filled circles, $N = 16$) and surface sediment (open circles, $N = 11$) from the Chesapeake Bay. Error bars for δD_{dino} and δD_{water} represent the standard deviation of three measurements as listed in Tables 1 and 2. Linear regressions for suspended particles (solid lines) and sediments (dotted lines) shown with 95% confidence intervals.

10 years, based on a linear sedimentation rate of $0.1\text{--}1 \text{ cm yr}^{-1}$ (Colman and Bratton, 2003)) accumulation of dinosterol produced in summer when surface water δD values are expected to be relatively high due to the diminished freshwater input. Concomitant higher surface salinities in summer relative to the rest of the year are also likely to contribute to the higher slope of the δD_{dino} vs. δD_{water} regression in sediment as compared to particles (Fig. 3a), as discussed below.

The slope and intercept of the linear regressions in Fig. 3a provide two expressions of the D/H fractionation (Sessions and Hayes, 2005) associated with dinosterol synthesis, α_{slope} and $\epsilon_{\text{intercept}}$, respectively. $\epsilon_{\text{intercept}}$ values can be converted to $\alpha_{\text{intercept}}$ values according to the relationship $\alpha_{\text{intercept}} = (\epsilon_{\text{intercept}}/1000) + 1$, resulting in $\alpha_{\text{intercept}}$ of 0.718 ± 0.004 for particulate dinosterol and 0.745 ± 0.004 for sedimentary dinosterol. These values are much lower than the α_{slope} values of 1.35 ± 0.15 and 1.91 ± 0.15 for particulate and sedimentary dinosterol, respectively. Furthermore, linear regression analysis of individual $\alpha_{\text{dino/water}}$

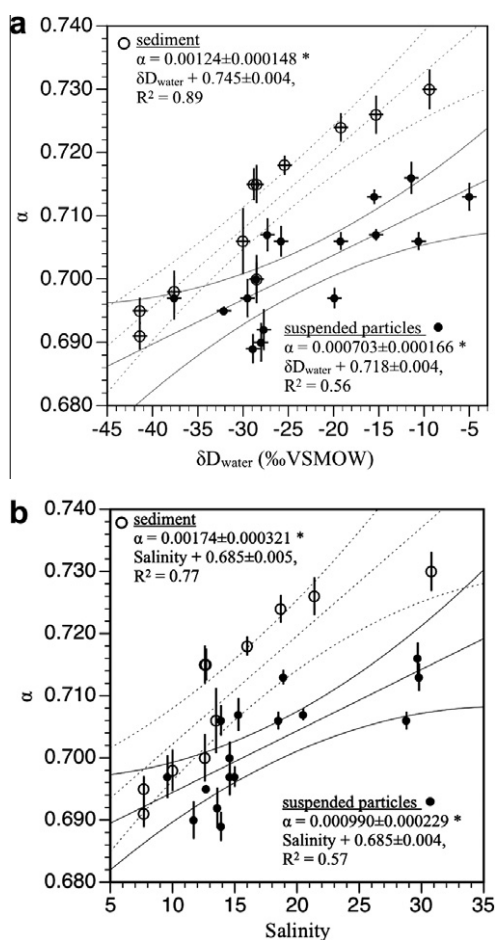


Fig. 4. $\alpha_{\text{dinosterol/water}}$ values in suspended particles (filled circles, $N=16$) and surface sediment (open circles, $N=11$), plotted against (a) δD_{water} and (b) salinity. Error bars for $\alpha_{\text{dino/water}}$ represent propagated errors reported for δD_{dino} and δD_{water} measurements, and error bars for δD_{water} are as in Fig. 3. Linear regressions for suspended particles (solid lines) and sediments (dotted lines) shown with 95% confidence intervals.

values onto δD_{water} values (Table 2) produces a positive slope of 0.000703 ± 0.000166 alpha units/‰ for suspended particles and 0.00124 ± 0.000148 alpha units/‰ for surface sediments (Fig. 4a). This positive slope implies that other parameters that are positively correlated with δD_{water} in the CB influence D/H fractionation in dinosterol. We propose that salinity is the most important such parameter, and that its effect on D/H fractionation during dinosterol biosynthesis causes just over half of the positive slope of the linear regression of δD_{dino} onto δD_{water} (Fig. 3a) and most of the positive slope of the linear regression of $\alpha_{\text{dino/water}}$ onto δD_{water} (Fig. 4a).

4.4. Influence of salinity on D/H fractionation in dinosterol

D/H fractionation in dinosterol decreased linearly as salinity increased in the CB (Fig. 4b). When regressed onto salinity $\alpha_{\text{dino/water}}$ values increased by 0.000990 ± 0.000229 (SE of regression slope) per unit increase in salinity in suspended particles and by 0.00174 ± 0.000321 per unit salin-

ity increase in surface sediments, both significant at the 95% confidence level (Fig. 4b). These values imply a decrease in D/H fractionation of 0.99 ± 0.23 ‰ per unit increase in salinity when measured in suspended particles and 1.7 ± 0.32 ‰/PSU when measured in surface sediments. Multiplying the 20.2 PSU increase in salinity (i.e., 9.6–29.8 PSU) in the region of the Bay from which the particulate dinosterol samples were taken by the 0.99 ± 0.23 ‰/PSU $\alpha_{\text{dino/water}}$ value for particles (Table 1) implies that 20 ± 4 ‰ (equivalent to 53%) of the total increase in δD_{dino} values in the CB can be attributed to the salinity increase.

That leaves $(38$ ‰ $- 20 \pm 4$ ‰) $= 18 \pm 4$ ‰, or 47% of the observed increase in δD_{dino} that can be attributed to a 33% increase in δD_{water} values, plus non-salinity influences on D/H fractionation during dinosterol biosynthesis. Factors other than salinity that have been demonstrated to influence D/H fractionation during lipid synthesis in plants and algae, or are suspected to, include: (i) nutrient-related growth rates (Zhang et al., 2009), (ii) water temperatures (which varied between 14.9° and 20.1 °C in this study; electronic annex, Fig. 1c) (Zhang et al., 2009), (iii) light levels, (iv) growth phase (Wolhowe et al., 2009), and (v) algal species cf. (Zhang and Sachs, 2007).

As discussed in Section 4.3, the higher slopes of the linear regressions of δD_{dino} onto both δD_{water} (Fig. 3a) and salinity (Fig. 3b), and $\alpha_{\text{dino/water}}$ onto both δD_{water} (Fig. 4a) and salinity (Fig. 4b) in sedimentary dinosterol relative to particulate dinosterol can be explained by high dinoflagellate production during summer when river flows and runoff are lowest. The particulate dinosterol and water samples were taken during high flow conditions in spring-time when surface water δD values and salinities in the CB are expected to be relatively low compared to the summer. In other words, the water overlying sediments in May is likely to be characterized by lower δD_{water} and salinity values than would typically occur in summer when dinoflagellate production peaks. Annual flux-weighted δD_{dino} values are thus expected to be higher than δD_{dino} values measured in May in response to the combined influence of higher δD_{water} values and diminished D/H fractionation in higher salinity water during summer.

An estimate of the fractionation factor for dinosterol biosynthesis at zero salinity is provided by the intercept of the linear regression of $\alpha_{\text{dino/water}}$ onto salinity, which is 0.685 for both particulate and sedimentary dinosterol (Fig. 4b). The resulting $\epsilon_{\text{dino/water}}$ value of -315 ‰ is within the range of previously reported values for isoprenoid lipids synthesized via the cytosolic mevalonate (MVA) pathway that span the range -142 ‰ to -376 ‰ (Sessions et al., 1999; Sauer et al., 2001; Zhang and Sachs, 2007). The fact that the y -intercept of the linear regression of $\alpha_{\text{dino/water}}$ onto salinity is nearly identical for both particulate and sedimentary dinosterol (0.6845 and 0.6848, respectively; Fig. 4b) suggests that 0.685 ($\epsilon_{\text{dino/water}} = -315$ ‰) is close to the true freshwater end-member of the ecosystem-integrated apparent fractionation factor for dinosterol biosynthesis.

The 0.99 ± 0.23 ‰ decrease in D/H fractionation per unit increase in salinity in particulate dinosterol is within 30% of the value determined for phytene (1.1 ‰/PSU),

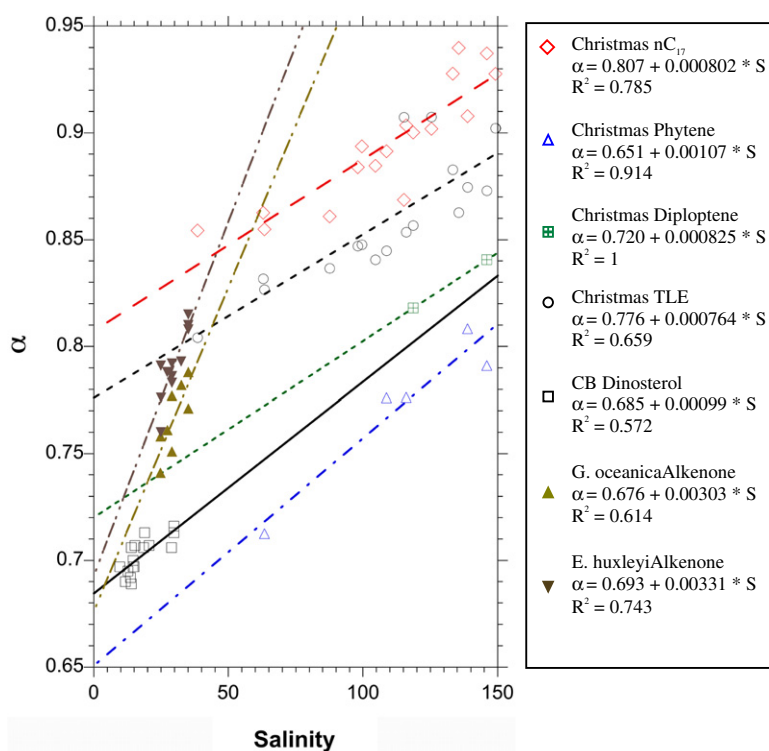


Fig. 5. $\alpha_{\text{lipid/water}}$ values for a variety of lipids from hypersaline ponds on Christmas Island (Sachse and Sachs, 2008) and from alkenones from cultured coccolithophorids (Schouten et al., 2006) are plotted along with the $\alpha_{\text{dino/water}}$ values from the Chesapeake Bay (this study).

nC_{17} alkane (0.80‰/PSU) and total lipid extracts (0.70‰/PSU) in hypersaline ponds on Christmas Island (Republic of Kiribati) by Sachse and Sachs (2008) (Fig. 5). Regardless of the biosynthetic pathway, environment, or source of the lipid, the D/H fractionation associated with salinity appears to be relatively constant in the diverse settings of the Chesapeake Bay estuary and the hypersaline ponds on Christmas Island.

These results are in conflict with those of Schouten et al. (2006) who reported a 3.3‰/PSU decrease in D/H fractionation as salinity increased in alkenones from batch cultures of *E. huxleyi* and *G. oceanica* (Schouten et al., 2006) (Fig. 5). The threefold greater sensitivity of D/H fractionation to changes in salinity in alkenones from batch cultures compared to a variety of acetogenic and isoprenoid lipids from Christmas Island and the CB remains unexplained. One possibility is that the “environmental” conditions within a batch culture can change substantially from the beginning to the end of an experiment, and the harvested cells integrate the response to all of those conditions, albeit with a bias toward those near the end of the experiment (owing to exponential growth). Light intensities (from self-shading), nutrient concentrations, growth rates, and the type and quantity of cellular metabolites all change during a batch culture experiment and many of these have either been shown explicitly to alter D/H fractionation in lipids, such as nutrient-induced growth rate changes (Zhang et al., 2009) or growth stage (Wolhowe et al., 2009), are likely to cause changes in growth rate or, in the case of light

intensity, to alter the δD value of hydrogen available for lipid biosynthesis (Luo et al., 1991; Schmidt et al., 2003).

4.5. Mechanism of salinity-induced D/H fractionation in dinosterol

We put forth three hypotheses to explain why increased salinity results in decreased D/H fractionation between dinosterol and extracellular water.

Hypothesis 1. Higher salinities cause decreased water transport across the cell membrane, resulting in greater recycling of internal water, and an increasingly D-enriched internal water pool from which lipids are synthesized (Kreuzer-Martin et al., 2006; Sachse and Sachs, 2008). Water transport across the cell membrane via aquaporins and Na^+ channels is restricted upon exposure to high salinities to prevent Na^+ toxicity (Pomati et al., 2004; Boursiac et al., 2005), while at the same time the volume of water in cyanobacterial cells has been shown to decline by up to 25% during salt stress (Allakhverdiev et al., 2000a,b). Lower transport rates of water across the cell wall, and a decreased pool of internal water would act in concert to continuously enrich the δD values of cellular water as NADPH is continuously replenished with D-depleted hydrogen. Estimates of the δD values of hydrogen for NADP+ protonation range from -250‰ to -600‰ (Luo et al., 1991; Schmidt et al., 2003). Lipids (and all other biosynthetic products) would reflect the increasingly elevated δD values characterizing the internal water.

Consequently it is possible that D/H fractionation between dinosterol and Chesapeake Bay water decreases from the headwaters to the mouth of the Bay as a result of decreased water transport across dinoflagellate cell membranes, diminution of their internal water pool, and an increase in the δD value of internal water as water is recycled rather than replenished from outside the cell, and D-depleted hydrogen is withdrawn for NADPH production.

Hypothesis 2. Elevated salinities cause growth rates to decline, resulting in diminished D/H fractionation between lipids and extracellular water. Many studies on phytoplankton and algae indicate that growth rates generally decrease upon exposure to elevated salinities (Herbst and Bradley, 1989; Clavero et al., 2000; Cifuentes et al., 2001). Though different algae are adapted to a range of optimal salinities, virtually all experience a decline in growth rate once a threshold salinity is passed. Laboratory culture studies on the marine diatom *Thalassiosira pseudonana* (Zhang et al., 2009) and the marine coccolithophorids *E. huxleyi* and *G. oceanica* (Schouten et al., 2006) indicate substantial decreases in D/H fractionation expressed in a variety of lipids as growth rates are reduced, either through purposeful nitrogen limitation (Zhang et al., 2009) or some combination of salinity and temperature (Schouten et al., 2006). If growth rates of dinosterol-producing dinoflagellates declined along the length of the CB it is possible that D/H fractionation between dinosterol and CB water decreased in concert.

Hypothesis 3. Upon exposure to high salinities rapid production of osmolytes draws D-depleted hydrogen from an internal pool of water, leaving it, and subsequent lipids synthesized from it, enriched in deuterium. When subjected to osmotic stress cells from all Domains of Life accumulate organic solutes to counteract the external osmotic pressure (Borowitzka and Brown, 1974; Brown, 1978; Reed et al., 1986; Galinski, 1995; Ventosa et al., 1998; Grant, 2004; Roberts, 2005). Also called osmolytes or compatible solutes (because they provide osmotic balance without interfering with the metabolic functions of the cell (Ventosa et al., 1998)) these small organic molecules span a wide diversity of structures and can be zwitterionic, uncharged or anionic (Roberts, 2005). Furthermore, they can represent a very substantial fraction of cellular hydrogen, reaching up to 10–20% of the dry weight of cells in some hypersaline bacteria (Ventosa et al., 1998). If hydrogen is shuttled off from internal pools of water and NADPH to rapidly synthesize osmolytes in response to osmotic stress, residual pools of those substances would be left enriched in deuterium, and all subsequent biosynthetic products would reflect this enrichment. Thus if dinoflagellates produce increasingly greater concentrations of osmolytes as salinities increase seaward in the Chesapeake Bay their internal pools of water and NADPH might become increasingly D-enriched, as would the dinosterol synthesized from that water, resulting in less D/H fractionation relative to CB water.

Both Hypotheses 1 and 3 call on a change in the internal water δD value as salinity changes, and would thus predict that all biosynthetic products would experience a decrease

in D/H fractionation relative to external water since water is the source of hydrogen for all biochemicals in phytoplankton. Hypothesis 2 calls upon a salinity-induced reduction in growth rate as the source of lowered D/H fractionation in dinosterol (and other lipids) relative to water, but does not necessarily predict that all biosynthetic products be increased in δD . These are testable hypotheses that future work ought to address.

4.6. Outlook for paleoclimate studies

Data from the Chesapeake Bay make a strong case for the use of sedimentary dinosterol δD values as both qualitative and quantitative indicators of hydrologic changes in freshwater, brackish and saline systems.

It is now well established that a wide diversity of lipids record δD values that track δD_{water} values with near perfection ($R^2 > 0.99$) in cultured marine and freshwater microalgae (Englebrecht and Sachs, 2005; Schouten et al., 2006; Zhang and Sachs, 2007). Because rain and runoff have low δD values compared to seawater (Craig and Gordon, 1965a; Gat, 1996), dinosterol produced in freshwater will have a low δD value reflecting the low δD_{water} values and maximal D/H fractionation relative to environmental water when salinity is zero. In a brackish lake, lagoon or estuary, δD_{water} values will increase as the fraction of seawater increases, resulting in higher δD values of dinosterol. Amplifying the signal and further elevating the δD value of dinosterol produced in brackish water will be a decrease in D/H fractionation during dinosterol biosynthesis in response to saltier environmental water. In this fashion both salinity and water isotopic changes will act in concert to elevate dinosterol δD values. In other words the ‘salinity effect’ on dinosterol δD values amplifies the ‘water effect’. In an estuary or a brackish lake or lagoon, temporal changes in the relative proportion of freshwater and seawater can therefore be sensitively, albeit qualitatively, evaluated from down-core sedimentary δD_{dino} values.

An additional amplifying influence on the δD_{dino} hydrologic proxy in low latitudes will be the so-called ‘amount effect’ in which greater precipitation amounts (on a variety of time scales) are associated with lower δD (and $\delta^{18}\text{O}$) values of that precipitation (Dansgaard, 1964; Rozanski et al., 1993; Johnson and Ingram, 2004; Sturm et al., 2007; Kurita et al., 2009). This effect is large in tropical marine locations where convective rainfall is prevalent. For example, $d\delta D_{\text{precip}}/dP \sim -0.1\text{‰}/\text{mm}$ when the precipitation amount P (in mm) and δD_{precip} are the long-term monthly mean values on tropical islands (Kurita et al., 2009). The large vertical component of such air masses progressively depletes the precipitation in D. This effect can be amplified by reduced isotopic exchange between raindrops and water vapor and reduced evaporative enrichment of deuterium in heavy rain events (Johnson and Ingram, 2004). Thus a 35% reduction in rainfall in the western tropical Pacific island nation of Palau, from 300 to 200 mm/month, is associated with a 10‰ increase in the monthly mean δD value of precipitation (Kurita et al., 2009). In a brackish system this effect will be additive with the ‘water effect’ (in which seawater has higher δD_{water} than freshwater) and the ‘salinity

effect' (in which less D/H fractionation occurs in lipids when external water salinity increases). Acting in concert these three effects make the δD_{dino} signal a sensitive qualitative indicator of hydrologic conditions in tropical saline systems, with higher δD_{dino} values reflecting saltier and/or drier conditions, and lower δD_{dino} values reflecting fresher and/or wetter conditions.

Temporal and spatial changes in the salinity of ocean surface waters are likely to be too small to substantially alter dinosterol and other algal lipid δD values because the direct effect of even a 5 PSU change in salinity – about the range of surface salinities in most of the modern ocean away from ice margins and rivers (Antonov et al., 2006) – would alter lipid δD values by about 4–5‰ (depending on the lipid) assuming $\sim 1\%$ per unit increase in salinity, which is close to the precision for lipid δD analyses with current analytical techniques. However, with a larger salinity effect, such as the $\sim 3\%$ per unit increase in salinity reported for alkenones by Schouten et al. (2006), or in those locations where a very large salinity change is possible, such as near rivers and in ice proximal locations, temporal changes in surface ocean salinity may be large enough to cause a detectable change in lipid D/H fractionation.

A high correlation between particulate δD_{dino} and δD_{water} values in the CB where substantial changes in the dinoflagellate assemblage occurs along the gradient from oligohaline to mesohaline to polyhaline waters (Marshall et al., 2006; Marshall et al., 2009) implies that any species-specific differences in D/H fractionation during dinosterol synthesis are a second order influence on δD_{dino} values in the CB estuary compared to the influence of salinity. Extrapolating this spatial observation to the time domain would imply that paleohydrologic reconstructions from sedimentary δD_{dino} values ought to be relatively insensitive to temporal changes in environmental conditions above a core site that could alter the dinoflagellate assemblage. This is important because up to 100‰ differences have been observed in the δD values of identical lipids from different genera, and 10–15‰ differences between species of the same genus, of green algae grown in freshwater with the same δD value (Zhang and Sachs, 2007). The high correlation between dinosterol δD , $\alpha_{\text{dino/water}}$, and both salinity and δD_{water} further attests to the promise of the δD_{dino} paleohydrologic and paleosalinity proxy. A similar inference was drawn from lipid δD values in dozens of saline and hypersaline ponds on Christmas Island in the central equatorial Pacific, where a suite of different lipids and even total lipid extracts were found to have δD values highly correlated with salinity (Sachse and Sachs, 2008). Again this suggests the lipid δD salinity and hydrologic proxy may be robust across species and environments.

Applying the modern-system spatial calibration to understand the past as described above requires the added assumption that either no changes in the δD values of the source precipitation have occurred, or that if they have, they are related to hydrologic factors that are easily interpretable. Many locations in the tropics meet these criteria. In tropical locations that are far enough away from the influence of large landmasses, the dominant cause of isotopic variability on average monthly and annual timescales is

the amount effect (Kurita et al., 2009). This makes these locations ideal sites for application of δD values in aquatic lipids because competing influences on the δD values of source waters are unlikely.

Finally, quantitative determinations of salinity and δD_{water} values from down-core sedimentary δD_{dino} values ought to be possible using the equations relating those parameters in the CB (Fig. 3) provided that the local relationship between δD_{water} and salinity is similar to that in the CB. If the local δD_{water} -salinity relationship differs substantially from the CB relationship ($\delta D_{\text{water}} = 1.63 \times \text{Sal} - 52.2$) then a local calibration of either δD_{water} or δD_{dino} vs. salinity is required. Furthermore, we advise using the equations derived from dinosterol in the CB particles rather than the sediments (Fig. 3). Dinosterol in the particles was presumably produced in the water from which those particles were filtered, the same water used for δD_{water} analyses. Dinosterol in surface sediments was produced over months to years and at a variety of water depths, salinities and δD_{water} values. The latter are likely to vary seasonally and perhaps annually. Yet we used δD_{water} values measured at 3 m in May 2006, the approximate depth of highest productivity to calculate α values. This difference in the time and depth over which the surface sediment and water samples integrate would yield δD_{water} values derived from sedimentary δD_{dino} values using the “sediment equation” representative of something akin to May 2006 conditions. The “particle equation” ought to yield δD_{water} values associated with the mean conditions over which the dinosterol extracted from a sediment sample was produced.

5. CONCLUSION

An investigation of the hydrogen isotopic composition of the dinoflagellate sterol dinosterol in suspended particles and sediments of the Chesapeake Bay estuary indicates that the isotopic composition of water and a biological response to salinity contribute equally to δD_{dino} changes. D/H fractionation during dinosterol synthesis decreased by $0.99 \pm 0.23\%$ per unit increase in salinity along the Bay. This decrease in fractionation is similar to that observed in several lipids from hypersaline ponds on Christmas Island (Kiribati) reported by Sachse and Sachs (2008), but is only 30% of the decrease observed in alkenones from batch-cultured coccolithophorids by Schouten et al. (2006). D/H fractionation during dinosterol biosynthesis at zero salinity is estimated to be -315% , which is within the range of previously reported values for isoprenoid lipids synthesized via the cytosolic mevalonate (MVA) pathway.

Three hypotheses are presented to explain the sensitivity of D/H fractionation in dinosterol to salinity changes, none or all of which may act to cause a decrease in D/H fractionation as salinity increases. The first possibility is that higher salinities result in decreased water transport across cell membranes, greater recycling of internal water, and an increasingly D-enriched internal water pool from which lipids are synthesized. The second hypothesis is that elevated salinities cause growth rates to decrease, resulting in diminished D/H fractionation between lipids and extracellular water. The third hypothesis is that compatible solutes

known as osmolytes are produced in great abundance upon exposure to high salinities, drawing substantial quantities of D-depleted hydrogen from an internal pool of water, leaving it, and the lipids synthesized from it, enriched in deuterium.

The high correlation between δD_{dino} values in particles and sediments from the Chesapeake Bay and δD_{water} and salinity permits the estimation of salinity and δD_{water} values in the past from sedimentary δD_{dino} values in locations that have a similar δD_{water} –salinity relationship. The calibrations derived from suspended particles, which are $\delta D_{\text{dino}} = 1.35 \pm 0.15 \times \delta D_{\text{water}} - 283 \pm 4$ ($R^2 = 0.85$, $N = 16$) and $\delta D_{\text{dino}} = 1.80 \pm 0.26 \times \text{salinity} - 345 \pm 5$ ($R^2 = 0.77$, $N = 16$), ought to be used instead of those derived from surface sediments since dinosterol in the upper 0–2 cm of sediment was likely deposited over months or years while the δD_{water} and salinity data were from a brief period of time in May 2006.

ACKNOWLEDGEMENTS

This material is based upon work supported by the National Science Foundation under Grants ESH-0639640, EAR-0745982 and EAR-0823503; the American Chemical Society through Petroleum Research Fund grant 46937-AC2; and by the Gary Comer Science and Education Foundation. The Swiss National Science Foundation provided financial support to V. Schwab through a postdoctoral fellowship. We are grateful to Dan Nelson for editing and improving the manuscript. We thank Alyssa Atwood, Jeff Bowman, Dirk Sachse, Rienk Smittenberg, and Guillaume Leduc for thoughtful discussions. The comments of Associate Editor Jaap Sinninghe Damsté, Kate Freeman and two anonymous reviewers strengthened the manuscript significantly. We thank Rienk Smittenberg, Orest Kawka, Dirk Sachse and Zhaohui Zhang for assistance in the laboratory, and Rienk Smittenberg and Dirk Sachse for assistance in the field. We are grateful to the Virginia and Maryland Chesapeake Bay Monitoring Programs for making their research vessels and facilities available to us, and to Rick Younger, captain of the *R/V Kerhin* from which many of the Chesapeake Bay samples were collected. We thank Ulrich Weber from the Biogeochemical Model-Data Integration Group (SNWG) at the Max-Planck-Institute for Biogeochemistry in Jena, Germany for assistance making the contour maps in Fig. 1.

APPENDIX A. SUPPLEMENTARY DATA

Supplementary data associated with this article can be found, in the online version, at [doi:10.1016/j.gca.2010.10.013](https://doi.org/10.1016/j.gca.2010.10.013).

REFERENCES

- Alam M., Sanduja R., Watson D. A. and Loeblich, III, A. R. (1984) Sterol distribution in the genus *Heterocapsa* (Pyrrophyta). *Journal of Phycology* **20**, 331–335.
- Allakhverdiev S. I., Sakamoto A., Nishiyama Y., Inaba M. and Murata N. (2000a) Ionic and osmotic effects of NaCl-induced inactivation of photosystems I and II in *Synechococcus* sp.. *Plant Physiology* **123**, 1047–1056.
- Allakhverdiev S. I., Sakamoto A., Nishiyama Y. and Murata N. (2000b) Inactivation of photosystems I and II in response to osmotic stress in *Synechococcus*. Contribution of water channels. *Plant Physiology* **122**, 1201–1208.
- Amo M., Suzuki N., Kawamura H., Yamaguchi A., Takano Y. and Horiguchi T. (2007) Biomarker compositions of dinoflagellates and their applications for paleoenvironmental proxies. In *The Origin and Evolution of Natural Diversity* (eds. H. Okada, S. F. Mawatari, N. Suzuki and P. Gautam). 21st Century COE for NEO-Science of Natural History, Hokkaido University, Sapporo, Japan.
- Antonov J. I., Locarnini R. A., Boyer T. P., Mishonov A. V. and Garcia H. E. (2006) *World Ocean Atlas 2005, volume 2: salinity*. US Government Printing Office, Washington, DC.
- Austin J. A. (2004) Estimating effective longitudinal dispersion in the Chesapeake Bay. *Estuarine, Coastal and Shelf Science* **60**, 359–368.
- Boon J. J., Rijpstra W. I. C., De Lange F. and De Leeuw J. W. (1979) Black Sea sterol – a molecular fossil for dinoflagellate bloom. *Nature* **277**, 125–127.
- Borowitzka L. J. and Brown A. D. (1974) The salt relations of marine and halophilic species of the unicellular green alga, *Dunaliella*. *Archives of Microbiology* **96**, 37–52.
- Boursiac Y., Chen S., Luu D. T., Sorieul M., van den Dries N. and Maurel C. (2005) Early effects of salinity on water transport in Arabidopsis roots. Molecular and cellular features of aquaporin expression. *Plant Physiology* **139**, 790–805.
- Briffa K. R., Osborn T. J., Schweingruber F. H., Jones P. D., Shiyatov S. G. and Vaganov E. A. (2002) Tree-ring width and density data around the Northern Hemisphere: Part 1, local and regional climate signals. *The Holocene* **12**, 737–757.
- Brown A. D. (1978) Compatible solutes and extreme water stress in eukaryotic microorganisms. *Advances in Microbial Physiology* **7**, 181–242.
- Calvo E., Pelejero C., Logan G. A. and De Dekker P. (2004). Dust-induced changes in phytoplankton composition in the Tasman Sea during the last four glacial cycles. *Paleoceanography* **19**, PA2020. doi: 10.1029/2003PA000992.
- Campbell B. J., Li C., Sessions A. L. and Valentine D. L. (2009) Hydrogen isotopic fractionation in lipid biosynthesis by H₂-consuming *Desulfobacterium autotrophicum*. *Geochim. Cosmochim. Acta* **73**, 2744–2757.
- Chikaraishi Y. and Naraoka H. (2007) Delta C-13 and delta D relationships among three n-alkyl compound classes (n-alkanoic acid, n-alkane and n-alkanol) of terrestrial higher plants. *Organic Geochemistry* **38**, 198–215.
- Cifuentes A. S., Gonzalez M. A., Inostroza I. and Aguilera A. (2001) Reappraisal of physiological attributes of nine strains of *Dunaliella* (Chlorophyceae): growth and pigment content across a salinity gradient. *Journal of Phycology* **37**, 334–344.
- Clavero E., Hernandez M., Mariona, Grimalt J. O. and Garcia-Pichel F. (2000) Salinity tolerance of diatoms from thalassic hypersaline environments. *Journal of Phycology* **36**, 1021–1034.
- Colman S. M. and Bratton J. F. (2003) Anthropogenically induced changes in sediment and biogenic silica fluxes in Chesapeake Bay. *Geology* **31**, 71–74.
- Cook E. R., Meko D. M., Stahle D. W. and Cleaveland M. K. (1999) Drought reconstructions for the continental United States. *Journal of Climate* **12**, 1145–1162.
- Cook E. R., Woodhouse C. A., Eakin C. M., Meko D. M. and Stahle D. W. (2004) Long-term aridity changes in the Western United States. *Science* **306**, 1015–1018.
- Cooper S. R. and Brush G. S. (1991) Long-term history of Chesapeake Bay anoxia. *Science* **254**, 992–996.
- Craig H. (1961) Isotopic variations in meteoric waters. *Science* **133**, 1702–1703.
- Craig H. and Gordon L. (1965a) Deuterium and oxygen 18 variations in the ocean and the marine atmosphere. In *Proceedings of a Conference on Stable Isotopes in Oceanographic*

- Studies and Paleotemperatures* (ed. E. Tongiorgi). CNR-Laboratorio di Geologia Nucleare, Pisa.
- Craig H. and Gordon L. I. (1965b) Deuterium and oxygen 18 variations in the ocean and the marine atmosphere. In *Stable Isotopes in Oceanographic Studies and Paleotemperatures* (ed. E. Tongiorgi). V. Lischi, Pisa.
- Dansgaard W. (1964) Stable isotopes in precipitation. *Tellus* **16**, 436–447.
- Englebrecht A. C. and Sachs J. P. (2005) Determination of sediment provenance at drift sites using hydrogen isotopes and unsaturation ratios in alkenones. *Geochim. Cosmochim. Acta* **69**, 4253–4265.
- Estep M. F. and Hoering T. C. (1980) Biogeochemistry of the stable hydrogen isotopes. *Geochim. Cosmochim. Acta* **64**, 1197–1206.
- Flanagan L. B., Comstock J. P. and Ehleringer J. R. (1991) Comparison of modeled and observed environmental influences on the stable oxygen and hydrogen isotope composition of leaf water in *Phaseolus vulgaris* L.. *Plant Physiol.* **96**, 588–596.
- Galinski E. A. (1995) Osmoadaptation in bacteria. *Advances in Microbial Physiology* **37**, 272–328.
- Gat J. R. (1996) Oxygen and hydrogen isotopes in the hydrologic cycle. *Annual Reviews of Earth and Planetary Sciences* **24**, 225–262.
- Grant W. D. (2004) Life at low water activity. *Philosophical Transactions of the Royal Society of London. Series B: Biological Sciences* **359**, 1249–1267.
- Hanisch S., Ariztegui D. and Puttmann W. (2003) The biomarker record of Lake Albano, central Italy – implications for Holocene aquatic system response to environmental change. *Organic Geochemistry* **34**, 1223–1235.
- Harding L. W. and Perry E. S. (1997) Long-term increase of phytoplankton biomass in Chesapeake Bay, 1950–1994. *Marine Ecology Progress Series* **157**, 39–52.
- Hayes J. M. (2001) Fractionation of carbon and hydrogen isotopes in biosynthetic processes. *Rev Mineral Geochem* **43**, 225–277.
- Herbst D. B. and Bradley T. J. (1989) Salinity and nutrient limitations on growth of benthic algae from two alkaline salt lakes of the western Great Basin (USA). *Journal of Phycology* **25**, 673–678.
- Huang Y., Shuman B., Wang Y. and Webb, III, T. (2002) Hydrogen isotope ratios of palmitic acid in lacustrine sediments record late Quaternary climate variations. *Geology* **30**, 1103–1106.
- Ishiwatari R., Yamada K., Matsumoto K., Houtatsu M. and Naraoka H. (1999) Organic molecular and carbon isotopic records of the Japan Sea over the past 30 kyr. *Paleoceanography* **14**, 260–270.
- Johnson K. R. and Ingram B. L. (2004) Spatial and temporal variability in the stable isotope systematics of modern precipitation in China: implications for paleoclimate reconstructions. *Earth and Planetary Science Letters* **220**, 365–377.
- Kreuzer-Martin H. W., Lott M. J., Ehleringer J. R. and Hegg E. L. (2006) Metabolic processes account for the majority of the intracellular water in log-phase *Escherichia coli* cells as revealed by hydrogen isotopes. *Biochem.* **45**, 13622–13630.
- Kurita N., Ichiyangi K., Matsumoto J., Yamanaka M. D. and Ohata T. (2009) The relationship between the isotopic content of precipitation and the precipitation amount in tropical regions. *Journal of Geochemical Exploration* **102**, 113–122.
- Leblond J. D. and Chapman P. J. (2002) A survey of the sterol composition of the marine dinoflagellates *Karenia brevis*, *Karenia mikimotoi*, and *Karlodinium micrum* distribution of sterols within other members of the class Dinophyceae. *Journal of Phycology* **38**, 670–682.
- Luo Y.-H., Steinberg L., Suda S., Kumazawa S. and Mitsui A. (1991) Extremely low D/H ratios of photoproduct hydrogen by cyanobacteria. *Plant Cell Physiol.* **32**, 897–900.
- Malone T. C., Ducklow H. W., Peele E. R. and Pike S. E. (1991). Picoplankton carbon flux in Chesapeake Bay. *Marine Ecology Progress Series* **78**, 11–22.
- Mansour M. P., Volkman J. K., Jackson A. E. and Blackburn S. I. (1999) The fatty acid and sterol composition of five marine dinoflagellates. *Journal of Phycology* **35**, 710–720.
- Marshall H. G. (1980) Seasonal phytoplankton composition in the lower Chesapeake Bay and old plantation creek, Cape Charles, Virginia. *Estuaries* **3**, 207–216.
- Marshall H. G. and Nesius K. K. (1996) Phytoplankton composition in relation to primary production in Chesapeake Bay. *Marine Biology* **125**, 611–617.
- Marshall H. G., Lane M. F. and Nesius K. K. (2003) Long-term phytoplankton trends and related water quality trends in the lower Chesapeake Bay, Virginia. *USA Environmental Monitoring and Assessment* **81**, 349–360.
- Marshall H. G., Burchardt L. and Lacouture R. (2005) A review of phytoplankton composition within Chesapeake Bay and its tidal estuaries. *J Plankton Res* **27**, 1083–1102.
- Marshall H. G., Lacouture R. V., Buchanan C. and Johnson J. M. (2006) Phytoplankton assemblages associated with water quality and salinity regions in Chesapeake Bay, USA. *Estuarine, Coastal and Shelf Science* **69**, 10–18.
- Marshall H., Lane M., Nesius K. and Burchardt L. (2009) Assessment and significance of phytoplankton species composition within Chesapeake Bay and Virginia tributaries through a long-term monitoring program. *Environmental Monitoring and Assessment* **150**, 143–155.
- Menzel D., van Bergen P. F., Schouten S. and Damste J. S. S. (2003) Reconstruction of changes in export productivity during Pliocene sapropel deposition: a biomarker approach. *Palaeogeography Palaeoclimatology Palaeoecology* **190**, 273–287.
- Officer C. B., Biggs R. B., Taft J. L., Cronin L. E., Tyler M. A. and Boynton W. R. (1984) Chesapeake Bay anoxia: origin, development, and significance. *Science* **223**, 22–27.
- Pagani M., Pedentchouk N., Huber M., Sluijs A., Schouten S., Brinkhuis H., Damste J. S. S., Dickens G. R. and Scientists E. (2006) Arctic hydrology during global warming at the Palaeocene/Eocene thermal maximum. *Nature* **442**, 671–675.
- Pahnke K. and Sachs J. P. (2006). Sea surface temperatures of southern midlatitudes 0–160 kyr B.P. *Paleoceanography* **21**, PA2003. doi: 10.1029/2005PA001191.
- Pahnke K., Sachs J. P., Keigwin L. D., Timmermann, A. and Xie, S. -P. (2007). Eastern tropical Pacific hydrologic changes during the past 27,000 years from D/H ratios in alkenones. *Paleoceanography* **22**, PA4214. doi: 10.1029/2007PA001468.
- Place A. R., Bai X., Kim S., Sengco M. R. and Wayne Coats D. (2009) Dinoflagellate host-parasite sterol profiles dictate karlotoxin sensitivity. *Journal of Phycology* **45**, 375–385.
- Polissar P. J., Freeman K. H., Rowley D. B., McInerney F. A. and Currie B. S. (2009) Paleoaltimetry of the Tibetan Plateau from D/H ratios of lipid biomarkers. *Earth and Planetary Science Letters* **287**, 64–76.
- Pomati F., Burns B. and Neilan B. (2004) Use of ion-channel modulating agents to study cyanobacterial Na(+)-K(+) fluxes. *Biol. Proced. Online* **6**, 137–143.
- Reed R. H., Borowitzka L. J., Mackay M. A., Chudek J. A., Foster R., Warr S. R. C., Moore D. J. and Stewart W. D. P. (1986) Organic solute accumulation in osmotically stressed cyanobacteria. *FEMS Microbiol Lett* **39**, 51–56.
- Roberts M. F. (2005) Organic compatible solutes of halotolerant and halophilic microorganisms. *Sal. Syst.* **1**, 1–30.

- Robinson N., Eglinton G., Brassell S. C. and Cranwell P. A. (1984) Dinoflagellate origin for sedimentary 4[alpha]-methylsteroids and 5[alpha](H)-stanols. *Nature* **308**, 439–442.
- Robinson N., Cranwell P. A., Eglinton G. and Jaworski G. H. M. (1987) Lipids of four species of freshwater dinoflagellates. *Phytochemistry* **26**, 411–421.
- Rozanski K., Araguas-Araguas L. and Gonfiantini R. (1993) Isotopic patterns in modern global precipitation. In *Climate Change in Continental Isotopic Records – Geophysical Monograph* 78 (eds. P. K. Swart, K. C. Lohman, J. McKenzie and S. Savin). American Geophysical Union, Washington, DC.
- Sachs J. P., Sachse D., Smittenberg R. H., Zhang Z., Battisti D. S. and Golubic S. (2009) Southward movement of the Pacific intertropical convergence zone AD 1400–1850. *Nature Geoscience* **2**, 519–525.
- Sachse D. and Sachs J. P. (2008) Inverse relationship between D/H fractionation in cyanobacterial lipids and salinity in Christmas Island saline ponds. *Geochim. Cosmochim. Acta* **72**, 793–806.
- Sauer P. E., Eglinton T. I., Hayes J. M., Schimmelmann A. and Sessions A. L. (2001) Compound-specific D/H ratios of lipid biomarkers from sediments as a proxy for environmental and climatic conditions. *Geochim. Cosmochim. Acta* **65**, 213–222.
- Schefuss E., Schouten S. and Schneider R. R. (2005) Climatic controls on central African hydrology during the past 20,000 years. *Nature* **437**, 1003–1006.
- Schleucher J., Vanderveer P., Markley J. L. and Sharkey T. D. (1999) Intramolecular deuterium distributions reveal disequilibrium of chloroplast phosphoglucose isomerase. *Plant Cell Environ* **22**, 525–533.
- Schmidt H.-L., Werner R. A. and Eisenreich W. (2003) Systematics of 2H patterns in natural compounds and its importance for the elucidation of biosynthetic pathways. *Phytochemistry Reviews* **2**, 61–85.
- Schouten S., Ossebaar J., Schreiber K., Kienhuis M. V. M., Langer G., Benthien A. and Bijma J. (2006) The effect of temperature, salinity and growth rate on the stable hydrogen isotopic composition of long chain alkenones produced by *Emiliania huxleyi* and *Gephyrocapsa oceanica*. *Biogeosciences* **3**, 113–119.
- Schubel J. and Pritchard D. (1986) Responses of upper Chesapeake Bay to variations in discharge of the Susquehanna River. *Estuaries and Coasts* **9**, 236–249.
- Schubert, C. J., Villanueva, J., Calvert, S. E., Cowie, G. L., Rad, U. V., Schulz, H., Berner, U. and Erlenkeuser, H. (1998). Stable phytoplankton community structure in the Arabian Sea over the past 200,000 years. *Nature*.
- Schwab V. F. and Sachs J. P. (2009) The measurement of D/H ratio in alkenones and their isotopic heterogeneity. *Organic Geochemistry* **40**, 111–118.
- Sessions A. L. (2006) Seasonal changes in D/H fractionation accompanying lipid biosynthesis in *Spartina alterniflora*. *Geochim. Cosmochim. Acta* **70**, 2153–2162.
- Sessions A. L. and Hayes J. M. (2005) Calculation of hydrogen isotopic fractionations in biogeochemical systems. *Geochim. Cosmochim. Acta* **69**, 593–597.
- Sessions A. L., Burgoyne T. W., Schimmelmann A. and Hayes J. M. (1999) Fractionation of hydrogen isotopes in lipid biosynthesis. *Organic Geochemistry* **30**, 1193–1200.
- Sessions A. L., Burgoyne T. W. and Hayes J. M. (2001) Determination of the H-3 factor in hydrogen isotope ratio monitoring mass spectrometry. *Anal Chem* **73**, 200–207.
- Sessions A. L., Jahnke L. L., Schimmelmann A. and Hayes J. M. (2002) Hydrogen isotope fractionation in lipids of the methane-oxidizing bacterium *Methylococcus capsulatus*. *Geochim. Cosmochim. Acta* **66**, 3955–3969.
- Smith F. A. and Freeman K. H. (2006) Influence of physiology and climate on delta D of leaf wax *n*-alkanes from C-3 and C-4 grasses. *Geochim. Cosmochim. Acta* **70**, 1172–1187.
- Smith B. N. and Ziegler H. (1990) Isotopic fractionation of hydrogen in plants. *Bot. Acta* **103**, 335–342.
- Smittenberg R. H. and Sachs J. P. (2007) Purification of dinosterol for hydrogen isotopic analysis using high-performance liquid chromatography–mass spectrometry. *Journal of Chromatography A* **1169**, 70–76.
- Solomon S., Plattner G.-K., Knutti R. and Friedlingstein P. (2009) Irreversible climate change due to carbon dioxide emissions. *Proceedings of the National Academy of Sciences* **106**, 1704–1709.
- Sternberg L., Deniro M. J. and Ajie H. (1984) Stable hydrogen isotope ratios of saponifiable lipids and cellulose nitrate from cam, C-3 and C-4 plants. *Phytochemistry* **23**, 2475–2477.
- Sternberg L., Niro M. J. and Ajie H. O. (1986) Isotopic relationships between saponifiable lipids and cellulose nitrate prepared from red, brown and green algae. *Planta* **169**, 320–324.
- Sturm C., Hoffmann G. and Langmann B. (2007) Simulation of the stable water isotopes in precipitation over South America: comparing regional to global circulation models. *Journal of Climate* **20**, 3730–3750.
- Theissen K. M., Zinniker D. A., Moldowan J. M., Dunbar R. B. and Rowe H. D. (2005) Pronounced occurrence of long-chain alkenones and dinosterol in a 25,000-year lipid molecular fossil record from Lake Titicaca, South America. *Geochim. Cosmochim. Acta* **69**, 623–636.
- van der Meer M. T. J., Baas M., Rijpstra W. I. C., Marino G., Rohling E. J., Sinninghe Damstè J. S. and Schouten S. (2007) Hydrogen isotopic compositions of long-chain alkenones record freshwater flooding of the Eastern Mediterranean at the onset of sapropel deposition. *Earth and Planetary Science Letters* **262**, 594–600.
- van der Meer M. T. J., Sangiorgi F., Baas M., Brinkhuis H., Sinninghe Damstè J. S. and Schouten S. (2008) Molecular isotopic and dinoflagellate evidence for Late Holocene freshening of the Black Sea. *Earth and Planetary Science Letters* **267**, 426–434.
- Ventosa A., Nieto J. J. and Oren A. (1998) Biology of moderately halophilic aerobic bacteria. *Microbiol. Mol. Biol. Rev.* **62**, 504–544.
- Volkman J. K. (1986) A review of sterol markers for marine and terrigenous organic matter. *Organic Geochemistry* **9**, 83–100.
- Volkman J. K., Kearney P. and Jeffrey S. W. (1990) A new source of 4-methyl sterols and 5[alpha](H)-stanols in sediments: prymnesiophyte microalgae of the genus *Pavlova*. *Organic Geochemistry* **15**, 489–497.
- Volkman J. K., Barrett S. M., Dunstan G. A. and Jeffrey S. W. (1993) Geochemical significance of the occurrence of dinosterol and other 4-methyl sterols in a marine diatom. *Organic Geochemistry* **20**, 7–15.
- Volkman J. K., Barrett S. M., Blackburn S. I., Mansour M. P., Sikes E. L. and Gelin F. (1998) Microalgal biomarkers: a review of recent research developments. *Organic Geochemistry* **29**, 1163–1179.
- Withers N. (1983) Dinoflagellate sterols. In *Marine Natural Products: Chemical and Biological Perspectives* (ed. P. J. Scheuer). Academic Press, New York.
- Wolhowe M. D., Prahl F. G., Probert I. and Maldonado M. (2009) Growth phase dependent hydrogen isotopic fractionation in alkenone-producing haptophytes. *Biogeosciences* **6**, 1681–1694.
- Yakir D. (1992) Variations in the natural abundance of O-18 and deuterium in plant carbohydrates. *Plant Cell Environ* **15**, 1005–1020.

- Zhang Z. and Sachs J. P. (2007) Hydrogen isotope fractionation in freshwater algae: I. Variations among lipids and species. *Organic Geochemistry* **38**, 582–608.
- Zhang Z., Sachs J. P. and Marchetti A. (2009) Hydrogen isotope fractionation in freshwater and marine algae: II. Temperature and nitrogen limited growth rate effects. *Organic Geochemistry* **40**, 428–439.
- Ziegler H. (1989) Hydrogen Isotope fractionation in plant tissues. In *Stable Isotopes in Ecological Research* (eds. P. Rundel, J. R. Ehleringer and K. Nagy). Springer-Verlag.
- Zimmerman A. R. and Canuel E. A. (2000) A geochemical record of eutrophication and anoxia in Chesapeake Bay sediments: anthropogenic influence on organic matter composition. *Marine Chemistry* **69**, 117–137.

Associate editor: Jaap S. Sinninghe Damsté